Thermal instability of a cation-disordered $NdBa_2Cu_3O_7$ superconductor

Dmitry V. Peryshkov,[a] Eugene A. Goodilin,*[a,b] Igor A. Presnyakov,[b] Kirill V. Didenko,[b] Yuri D. Tretyakov,[a,b] Alexander Birkner[c] and Wolfgang Grünert[c]

[a] *Department of Materials Science, M. V. Lomonosov Moscow State University, 119992 Moscow, Russian Federation*
[b] *Department of Chemistry, M. V. Lomonosov Moscow State University, 119992 Moscow, Russian Federation. Fax: +7 095 939 0998; e-mail: goodilin@inorg.chem.msu.ru*
[c] *Department of Chemistry, Bochum University, D-44780 Bochum, Germany*

DOI: 10.1070/MC2004v014n04ABEH001966

The influence of Nd^{3+}/Ba^{2+} antisite disordering on local structural distortions and the thermal stability of neodymium–barium high-temperature cuprate superconductors are studied.

The anomalous peak effect phenomenon associated with the outstanding magnetic and electric properties of a $NdBa_2Cu_3O_7$ high-temperature superconductor results from flux pinning on nanoscale compositional fluctuations formed in a supersaturated solid solution due to its subsolidus decomposition or demixing.[1–5] In this work, the phase stability and the local structure of a famous $NdBa_2Cu_3O_z$ superconductor were analysed in the samples with different cation ordering.

Pseudocubic $Nd_{1+x}Ba_{2-x}(Cu_{0.97}{}^{57}Fe_{0.03})_3O_z$ samples (x = 0, 0.6) for a combined study by Mössbauer spectroscopy, TEM, thermal and chemical analyses were obtained by the freeze drying of aqueous solutions prepared from chemically pure $Nd(NO_3)_3{\cdot}6H_2O$, $Ba(NO_3)_2$ and $Cu(NO_3)_2{\cdot}xH_2O$ salts and single-isotope ^{57}Fe foil dissolved in nitric acid. The aqueous solution was sprayed in liquid nitrogen and cryogranules thus obtained were freeze-dried under vacuum by slowly rising the temperature from liquid nitrogen up to 40 °C for 4–5 days (SNH-15, Usifroid). The semifinal carbon-free bluish salt product was converted into a black oxide precursor by additional drying at 150 °C for 3–5 h with further fast decomposition at 750–950 °C for 30 min. A special two-step procedure was used to prepare pseudocubic Nd123 samples.[6–8] The first stage consisted in the preliminary annealing of 5 mm pellets of the oxide precursor at 750 °C for 15–70 h in air. The second step was re-grinding, pressing and short-term (2–5 h) annealing at 950–1000 °C on MgO plates in air followed by quenching in liquid nitrogen. The Fe content was fixed at 3 at% at copper positions to record better quality spectra and, at the same time, to avoid the clustering of Fe in the lattice.[9] A half of each powdered sample was isothermally oxidised at 350 °C for 40–50 h and finally furnace cooled in the same boat in dry oxygen. The oxygen content of the samples was found by iodometric titration and thermal analysis (Perkin–Elmer Pyris Diamond; temperature range, 20–1000 °C; heating and cooling rates, 5 K min^{-1}; standard, Al_2O_3; sample weight, 10–15 mg).

Routine X-ray powder diffraction experiments for phase identification were carried out within the 2θ range 20–70° with a step of 0.03° (STOE diffractometer, $CuK\alpha_1$). Lattice constants were determined using powdered samples with finely dispersed germanium as an internal standard (FR-552 monochromator chamber, $CuK\alpha_1$) followed by the standard least-squares calculation procedure. The sample microstructures were studied using either scanning electron microscopy (JEOL 840 EPMA) combined with microanalysis or transmission electron microscopy (TEM) combined with selected area electron diffraction (JEOL 2000FX, Japan). AC susceptibility measurements for T_c determination were performed in applied fields of 10 Oe at 27 Hz within the temperature range 17–100 K (APD-Cryogenics). The temperature was screened by a controller from Scientific Instruments Inc. (series 5500). ^{57}Fe Mössbauer spectra were measured at room temperature using an electrodynamic spectrometer with a constant acceleration. The radiation source was $^{57}Co(Rh)$. The actual isomer shifts were adjusted according to α-Fe. Defect structure simulation was performed using the General Utility Lattice Program (GULP) software with input parameters adopted from refs. 10 and 11.

Table 1 Lattice constants of $Nd_{1+x}Ba_{2-x}Cu_3O_z$:^{57}Fe single phase samples.

Compound	*a*/Å	*b*/Å	*c*/Å
$NdBa_2(Cu_{0.97}{}^{57}Fe_{0.03})_3O_{6.93(1)}$			
produced at 980 °C (T_c = 56 K)	3.901(1)	3.901(1)	11.716(1)
produced at 850 °C[a]	3.906(1)	3.902(1)	11.698(2)
'ideal'[4,5] $NdBa_2Cu_3O_{6.90}$	3.916–3.918	3.858–3.868	11.745–11.772
'abnormal'[4,5] $NdBa_2Cu_3O_{6.88}$	3.902–3.908	3.896–3.899	11.706–11.719

[a]Non-superconducting.

The transfer of cations in a certain stoichiometric ratio from a water solution with almost molecular mixing of reagents into final ceramics makes freeze-drying one of the most effective methods to produce chemically homogeneous complex phases at the lowest temperatures.[4,5] Fully oxygenated XRD – pure $NdBa_2Cu_3O_{6.9}$:^{57}Fe samples demonstrated superconductivity transition temperatures drastically dropping down if the preparation temperature is set below 900 °C (Table 1). We found that such a discrepancy in T_c is accompanied by a specific difference in the XRD patterns of the samples, namely, single pseudocubic phases with almost equal *a*, *b* and *c*/3 parameters form below 900–950 °C (Table 1). This is a sign of cation re-distribution within a crystal lattice, as we detected earlier by EXAFS, XRD and Raman scattering spectroscopy.[4,6–8] An intermediate low-temperature treatment may predetermine a low T_c in Nd123 samples, especially for chemically homogenised submicron-particle precursors. The two-stage treatment described above allowed us to obtain for the first time intentionally and reproducibly pseudocubic neodimium–barium cuprates with the 1:2:3 stoichiometry.

Possible reasons for the unusual behaviour of pseudocubic phases can be revealed after the analysis of fitting parameters of Mössbauer spectra (Table 2). The hyperfine parameters of

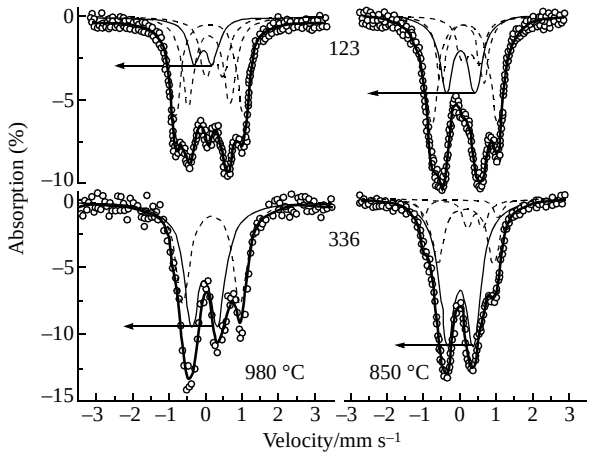

Figure 1 Mössbauer spectra of pairs of fully oxygenated $Nd_{1.6}Ba_{1.4}$-$(Cu_{0.97}{}^{57}Fe_{0.03})_3O_{7.29(1)}$ (336) and $NdBa_2(Cu_{0.97}{}^{57}Fe_{0.03})_3O_{6.93(1)}$ (123) samples of the same composition produced at different temperatures in air (850 or 980 °C). The D2 component is drawn by a thick solid curve.

the D1, D3, and D4 components correlate well with reference data.[6,9,12] The D3 component corresponds to tetravalent iron in the Cu(1) position with a planar rhombic oxygen configuration [$Fe^{IV}_{Cu(1)}O_4$]. The D1 component matches a pyramidal oxygen shell of trivalent iron at the same copper site ['$Fe^{III}_{Cu(1)}O_5$']. The D4 component looks alike '$Fe^{III}_{Cu(2)}O_6$' octahedra in the Cu(2) planes distorted because of the displacement of the apical oxygen atom O(3).

A specific feature of both pseudocubic Nd123 and the substituted solid solution is the existence of D2 component (Figure 1) never observed for the reference $YBa_2Cu_3O_z$ compound and associated with iron atoms at Cu(1) sites. A small value of quadrupole splitting of D2 itself might allow the assignment of D2 to an octahedral configuration in this particular case of rare-earth barium cuprates.[6] Hommonay reported[9] only highly symmetrical octahedra with iron(III) at Cu(1) sites, while the D2 component corresponds to distorted octahedra with formally tetravalent iron in the same position. It is evident that the D2 component appears due to neodymium-for-barium substitution since its contribution directly increases along with x for both quenched and oxidised solid solution samples (Table 2). The $Fe^{IV}_{Cu(1)}O_6$ octahedra are deformed as a result of asymmetry of the second coordination sphere since the second-order neighbours around them could be either barium atoms in their own positions or neodymium. The increase of the iron oxidation state for the D2 component can be explained by the formation of a $Fe^{IV}_{Cu(1)}O_6$–Nd_{Ba} defect associate. In this case, the O(4) oxygen atom, supplementing the iron six-fold coordination, is stabilised by neodymium in the barium position demanding the occupation of former vacancy chains by oxygens. A hole in this case does not transfer into the $Cu(2)O_2$ plane or onto Nd_{Ba} defects; preferably, it is caught by iron atoms in valence-saturated polyhedra forcing ^{57}Fe to be formally tetravalent. Therefore, the small isomer shift and relatively large quadrupole splitting are both reasonable for the D2 component making the D2 component a fingerprint of substituted neodymium–barium cuprates.

The c parameter of Nd123:Fe and Nd336:Fe phases becomes evidently smaller after their preparation at a lower temperature; such a Nd123:Fe sample demonstrates strongly suppressed superconducting properties after complete oxygenation (Table 1). The reason is a pronounced contraction of a charge reservoir block in the structure if a smaller Nd^{3+} ion enters the Ba^{2+} site and extra-oxygen is caught by the FeO_6–Nd_{Ba} defect associates. T_c suppression could also be caused by substantial local distortions around Nd_{Ba} as found by EXAFS and simulation with

Table 2 Mössbauer spectra parameters of $Nd_{1+x}Ba_{2-x}(Cu_{0.97}{}^{57}Fe_{0.03})_3O_z$ samples.

^{57}Fe-doped phases	Sub-spectra	Isomer shift, δ/mm s^{-1}	Quadrupole splitting, Δ/mm s^{-1}	Area (%)	Width, Γ/mm s^{-1}
$Nd_1Ba_2Cu_3O_{6.25}$	D1	0.08(0)	1.11(1)	12.3	0.39(0)
(quenching from 980 °C)	D2	**0.02(0)**	**0.50(1)**	**12.9**	**0.30(1)**
	D3	0.14(0)	1.89(0)	59.6	0.39(0)
	D4	0.25(0)	0.45(1)	15.2[a]	0.39(0)
$Nd_1Ba_2Cu_3O_{6.93}$	D1	0.08(0)	1.15(1)	32.1	0.39(0)
(980 °C, oxygenated)	D2	**–0.07(1)**	**0.50(2)**	**15.7**	**0.39(0)**
	D3	0.10(0)	1.86(1)	33.1	0.35(1)
	D4	0.25(0)	0.47(1)	19.1[a]	0.36(1)
$Nd_1Ba_2Cu_3O_{6.9}$	D1	0.07(1)	1.19(4)	18.8	0.32(5)
(850 °C, oxygenated)	D2	**0.02(1)**	**0.79(6)**	**27.9**	**0.44(4)**
	D3	0.12(0)	1.80(1)	39.5	0.40(2)
	D4	0.29(5)	0.44(6)	13.7	0.38(4)
$Nd_{1.6}Ba_{1.4}Cu_3O_{7.03}$	D1′	0.19(0)	1.55(1)	77.3	0.44(1)
(quenching from 980 °C)	D2′	**–0.01(1)**	**0.44(3)**	**22.7**	**0.42(3)**
$Nd_{1.6}Ba_{1.4}Cu_3O_{7.29}$	D1′	0.14(1)	1.58(1)	42.8	0.42(1)
(980 °C, oxygenated)	D2′	**–0.04(1)**	**0.72(1)**	**57.2**	**0.49(1)**
$Nd_{1.6}Ba_{1.4}Cu_3O_{7.3}$	D1′	0.17(1)	1.52(1)	24.1	0.40(4)
(850 °C, oxygenated)	D2′	**0.00(0)**	**0.71(1)**	**65.3**	**0.50(2)**
	D3	0.04(1)	2.05(2)	3.7	0.20(4)
	D4	0.42(1)	0.45(2)	6.8	0.24(2)

[a]The difference in contributions is equal to the contribution of magnetic subspectrum disappearing after oxygenation.

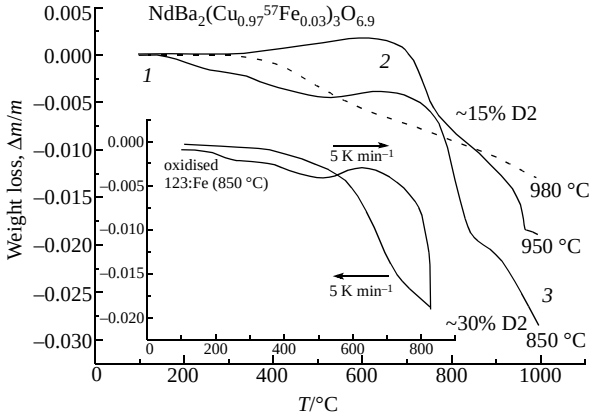

Figure 2 Thermal analysis data of oxygenated iron-doped $NdBa_2(Cu_{0.97}{}^{57}Fe_{0.03})_3O_{6.9}$ samples initially prepared at 850, 950 or 980 °C and heated in air with a constant rate of 5 K min^{-1}. (*1*) The beginning of weight lost by cation-disordered samples, (*2*) weight gain due to solid state decomposition, (*3*) an abrupt weight change at high temperatures. Inset shows thermal cycling of an independently measured sample synthesised at 850 °C.

GULP.[10,11] The Mössbauer spectra of both Nd123:Fe and Nd336:Fe samples also confirm that the sample preparation history is important since it affects the local structure. In both the cases, an increase of the preparation temperature decreases the contribution of the D2 component (Figure 1). These results prove the possibility of a partial antisite exchange of neodymium and barium between their crystallographic positions. This is the only assumption that preserves an overall Nd:Ba:Cu = 1:2:3 phase composition, results in the reduction of c parameter of the unit cell and its orthorhombicity due to extra oxygen atoms in the former vacancy chains and local distortions of perovskite-like blocks.

The TGA curves of fully oxygenated pseudocubic Nd123 samples are unusual since they demonstrate an increase of the sample weight on heating (Figure 2). This is a reproducible phenomenon since it is present in several pseudocubic samples produced at different temperatures and also in samples of a different series obtained at 850 °C (Figure 2, see also ref. 8 for samples without iron doping). The weight gain is irreversible since heating and cooling curves are different (Figure 2, inset). Therefore, it is an evidence for a non-equilibrium process occurring in a solid state during heating. This phenomenon is different from the normal behaviour of HTSC cuprates loosing oxygen at elevated temperatures; therefore, the state corresponding to a maximum on TGA curves (Figure 2, 650 °C) should be analysed. TEM proves (Figure 3) that grains of the neodymium–barium cuprate quenched from ~650 °C contain high-contrast regions and dark round-shaped inclusions embedded in the crystalline matrix. Such a microstructure can be explained by a solid-state process compatible with a picture of phase relations in the test system:[3–5] $NdBa_2Cu_3^{I,II}O_z + \gamma O_2 \rightarrow 1/(1+x)Nd_{1+x}Ba_{2-x}Cu_3^{II}O_{z_1} + 3x/(1+x)BaCuO_{2+\delta}$ ($x \sim 0.1$–0.15).

Computer simulation of defect energies (Table 3) and local distortions caused by antisite disorder confirms that such defects become less stable at a smaller oxygen content. It correlates well with findings on high-temperature ordering in this structure,[7,8] as well as with the formation mechanism of these defects in oxygen-deficient perovskites requiring extra oxygen to enter in the lattice to form the above associates of defects $Fe^{IV}_{Cu(1)}O_6$–Nd_{Ba} found by Mössbauer spectroscopy.[6] Therefore, the $NdBa_2Cu_3O_z$:Fe phase with Nd^{3+}/Ba^{2+} antisites decomposes as soon as oxygen

Table 3 Calculated energies of antisite defects in the $NdBa_2Cu_3O_z$ superconductor at different z.

z	Defect energy/eV
6.91	–1.85
6.77	–0.93
6.57	+0.16
6.52	+2.50

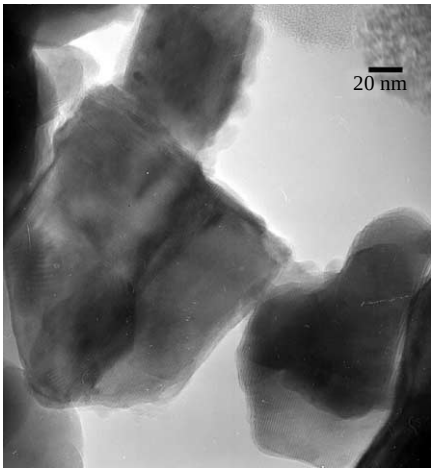

Figure 3 TEM micrograph of the $NdBa_2(Cu_{0.97}{}^{57}Fe_{0.03})_3O_{6.9}$ sample prepared at 850 °C, aged at 650 °C and quenched in liquid nitrogen.

content decreases and cation diffusivity reaches appreciable values, at ~650 °C (Figure 2).

Thus, the fundamental superconducting properties of neodymium–barium cuprates are preparation-dependent for a given cation and anion composition as a result of Nd/Ba cation disorder formed at lower annealing temperatures. A new spectral component characterised by an isomer shift of about 0 mm s^{-1} and quadrupole splitting of about 0.5 mm s^{-1} was found for all the cases of a substituted solid solution with $x > 0$ and also for the $x = 0$ pseudocubic Nd123:Fe phase. This evidences for the formation of associated defects like '$Fe^{IV}_{Cu(1)}O_6$–Nd_{Ba}' and confirms the antisite disordering of Nd^{3+} and Ba^{2+} in the low-T_c $NdBa_2Cu_3O_z$ samples. The latter type of samples is thermally unstable and undergoes solid-state decomposition at about 600–700 °C.

This work was supported by the Russian Foundation for Basic Research (grant nos. 04-03-32183 and 04-03-32827).

References

1 M. Murakami, N. Sakai, T. Higuchi and S. I. Yoo, *Supercond. Sci. Technol.*, 1996, **9**, 1015.
2 Y. Shiohara and A. Endo, *Mater. Sci. Engr.*, 1997, **R19**, 1.
3 Y. Shiohara and E. A. Goodilin, in *Handbook on the Physics and Chemistry of Rare-Earths*, eds. K. A. Gschneidner, Jr., L. Eyring and M. B. Maple, Elsevier Science, North-Holland, 2000, ch. 189, vol. 30, pp. 67–221.
4 Yu. D. Tret'yakov and E. A. Goodilin, *Russ. J. Inorg. Chem.*, 2001, **46**, S203.
5 Yu. D. Tretyakov and E. A. Goodilin, *Usp. Khim.*, 2000, **69**, 3 (*Russ. Chem. Rev.*, 2000, **69**, 1).
6 K. V. Didenko, D. V. Peryshkov, E. A. Gudilin, I. A. Presnyakov, E. A. Pomerantseva and Yu. D. Tret'yakov, *Dokl. Ross. Akad. Nauk*, 2002, **387**, 343 [*Dokl. Chem.* (*Engl. Transl.*), 2002, **387**, 316].
7 D. V. Peryshkov, E. A. Gudilin, M. V. Makarova, E. A. Pomerantseva, S. N. Mudretsova, A. F. Maiorova and Yu. D. Tret'yakov, *Dokl. Ross. Akad. Nauk*, 2002, **387**, 491 [*Dokl. Chem.* (*Engl. Transl.*), 2002, **387**, 323].
8 D. V. Peryshkov, E. A. Gudilin, M. V. Makarova, E. A. Trofimenko, S. N. Mudretsova, A. F. Maiorova and Yu. D. Tret'yakov, *Dokl. Ross. Akad. Nauk*, 2002, **383**, 651 [*Dokl. Chem.* (*Engl. Transl.*), 2002, **383**, 105].
9 Z. Hommonay, in *Mössbauer Spectroscopy of Sophisticated Oxides*, eds. A. Vertes and Z. Hommonay, Akademiai Kiado, Budapest, 1997, 159.
10 V. V. Petrykin, E. A. Goodilin, J. Hester, E. A. Trofimenko, N. N. Oleynikov, M. Kakihana and Yu. D. Tretyakov, *Physica C*, 2000, **340**, 16.
11 V. V. Petrykin, E. A. Goodilin, J. Hester, E. A. Trofimenko, M. Kakihana, N. N. Oleynikov and Yu. D. Tretyakov, *Physica C*, 2001, **357**, 388.
12 E. A. Gudilin, I. A. Presnyakov, M. V. Tarasov, S. N. Mudretsova, A. F. Maiorova, J. Hester, N. N. Oleinikov and Yu. D. Tret'yakov, *Dokl. Ross. Akad. Nauk*, 2000, **373**, 771 [*Dokl. Chem.* (*Engl. Transl.*), 2000, **373**, 160].

Received: 4th June 2004; Com. 04/2291